Direct structural transformation of silver platelets into right bipyramids and twinned cube nanoparticles: morphology governed by defects†

Matthew McEachran and Vladimir Kitaev*

Received (in Cambridge, UK) 5th August 2008, Accepted 4th September 2008
First published as an Advance Article on the web 1st October 2008
DOI: 10.1039/b813519c

Silver platelets can undergo quantitative conversion to right bipyramids and twinned cubes by regrowth with silver in conditions that preserve original 2-D structural defects in resulting 3-D morphologies.

Understanding and controlling metal nanoparticle (MNP) morphologies[1] is important for a wide range of practical applications in diverse scientific fields, such as catalysis,[2] biosensing,[3] plasmonics,[4] *etc*. To attain all the wealth of nanocrystal shapes analogous to crystal habits in mineralogy, the controlled incorporation and preservation of regular lattice defects is important since metals themselves feature a limited number of packing types. For instance, gold and silver, with their thermodynamically stable fcc lattices, can form defect-free nanoshapes of only cubooctahedral symmetries.[5] At present, several silver nanoshapes have been produced with control over twinning defects by an oxidative etching approach: pentagonal wires,[6] decahedra,[7] right bipyramids,[8] and platelets.[9] Silver platelets (triangular and hexagonal prisms) were established as one of the first well-defined silver NP morphologies.[10] Yet the exact nature of their structural defects has not been fully established, and only recent reports have brought more certainty in its understanding.[11,12]

While working on the nature of structural defects in silver platelets, we performed several experiments aimed at enlarging the platelets to better visualize their morphologies. Experimenting with the transformation parameters we discovered that in certain conditions we can stabilize AgNP (100) facets and thus attain a mixture of relatively monodisperse right bipyramids and twinned cubes. To date, no preparation of bipyramids in aqueous solutions has been reported, and to the best of our knowledge twinned cubes have not been described in the literature. Herein we report on the pathway of structural transformations of silver platelets to bipyramids and cubes in aqueous solutions elucidated by optical spectroscopy and electron microscopy.

Representative electron microscopy images of AgNPs formed by the transformation of silver platelets are shown in Fig. 1. The transformation involves rapid heating to near boiling of aqueous dispersions of silver platelets with silver nitrate in the presence of PVP and citrate ions. (More details are given in ESI†.) Rapid heating[13] assures the optimum preservation of the key feature crucial for the transformation: multiple twinning defects of the platelets.[11]

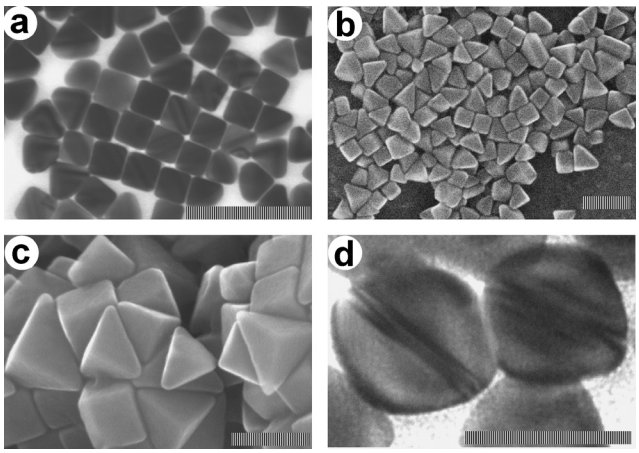

Fig. 1 Representative SEM and TEM images of silver right bipyramids and twinned cubes produced by direct transformation of silver platelets. The cube edge length and pyramidal base length are respectively: (a) 26 ± 2 and 37 ± 5 nm; (b) 39 ± 5 and 68 ± 6 nm; (c) 67 ± 4 and 99 ± 10 nm; (d) HRTEM of twinned defects in cubes. The scale bar is 100 nm for (a), (b) and (c) and 20 nm for (d).

It should be emphasized that the cubes and bipyramids are unambiguously a product of platelet transformation. Silver reduction in the absence of platelets but otherwise similar conditions takes significantly longer times (>15 *vs*. 3–4 min) and yields simply a variety of irregular shapes dominated by rod-like structures (Fig. S1a in ESI†) with appreciably broader red-shifted spectra compared to analogously produced cubes and bipyramids (Fig. S1b†). At the same time, if the platelets are heated in similar conditions without silver nitrate, they only can undergo decrease in lateral dimensions accompanied by an increase in thickness (Fig. S2†) and a resulting blue shift of the main plasmon resonance (spectrum ❷ in Fig. 2a).

By virtue of plasmon resonances of silver nanostructures spanning across the visible spectrum, the structural transformation of platelets to cubes and bipyramids is accompanied by prominent visual changes which can be conveniently monitored by UV-vis spectroscopy. Fig. 2 shows the sequence of changes upon transformation, separated into two parts for clarity: an initial blue shift of platelet compaction in the initial stages (Fig. 2a) and a subsequent red shift upon NP growth (Fig. 2b). The progression along the transformation path was controlled by adding different amounts of silver (kinetics of

Chemistry Department, Wilfrid Laurier University, 75 University Ave. W, Waterloo, Ontario, Canada N2L 3C5. E-mail: vkitaev@wlu.ca; Tel: +1-416-884-1970 ext. 3643

† Electronic supplementary information (ESI) available: Experimental, additional electron microscopy images, UV-vis and Raman spectra. See DOI: 10.1039/b813519c

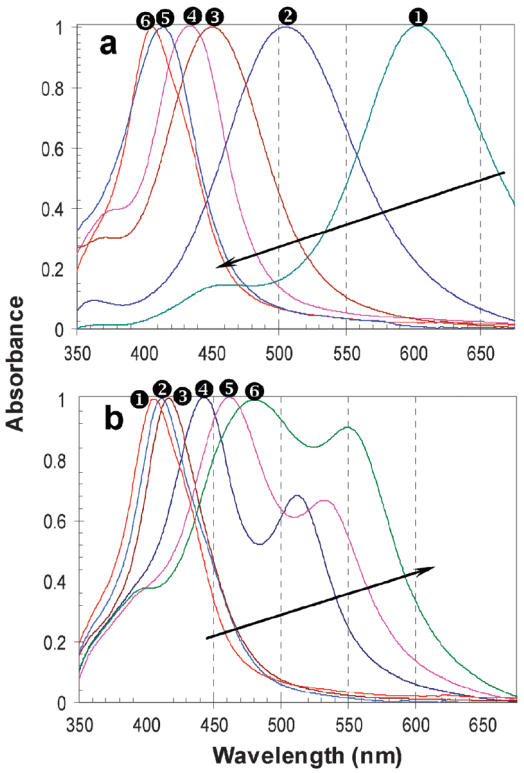

Fig. 2 (a) UV-vis spectra of silver platelet transformations into cubes and bipyramids Spectra are normalized and their maxima are labelled with circled symbols ❶ to ❻ for clarity. (a) Platelet compaction (blue shift). ❶: original platelets, ❷: platelets heated without silver for 4 min. The amounts of new silver added from ❸ to ❻ are 15%, 25%, 75% and 125% relative to that originally present in platelets. (b) Growth of small cubes and bipyramids in size upon progressive increase in added silver (red shift). The amounts of new silver added from ❶ to ❻ are 125%, 300%, 600%, 900%, 1200% and 1500% respectively.

the growth was also monitored for double control). Starting from the original blue platelet dispersions with their dominant plasmon resonance at around 600 nm, the main plasmonic peak first shifts rapidly to the blue reaching 407 nm upon addition of increasing amounts of silver (*ca.* 125%, as shown in Fig. 2a). The peak at 407 nm corresponds to the smallest size of cubes (*ca.* 15 nm) that could be observed during the platelet transformation. The peak shoulder of original and partly transformed prisms at 400–450 nm corresponds to quadrupole resonances.[10] The electron microscopy images of the transformation pathway are presented in Fig. 3. The original platelets are shown for comparison in Fig. 3a. Initial changes manifest in platelet thickening accompanied with a significant decrease in lateral dimensions (Fig. 3b). These changes correspond to the shift of the plasmonic peak from *ca.* 600 to 450 nm. (Fig. 2a). Then, the lateral decrease stops and bipyramids and cubes start to form at this stage. At this point the plasmonic peak is at its lowest at *ca.* 407 nm. Once this formation process is started, the growth of the cubes and bipyramids proceeds quite rapidly. Thus, rather than undergoing gradual growth of the platelets, a mixture of unconverted thickened platelets and small cubes and bipyramids is formed (Fig. 3c). The proportion of cubes and bipyramids in this mixture constantly increases upon further silver addition.

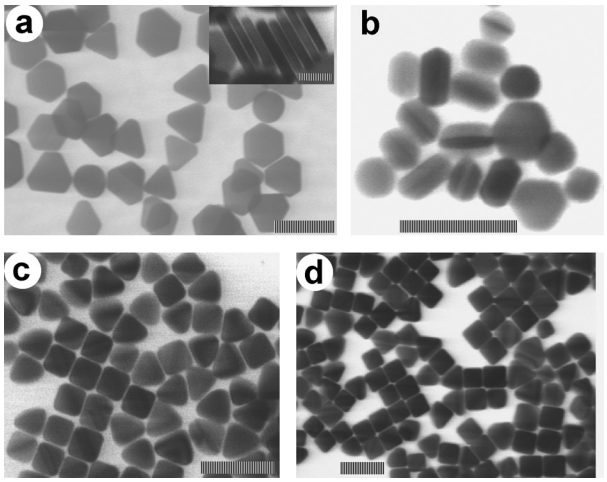

Fig. 3 SEM images illustrating the transformation pathway of platelets to cubes and right bipyramids: (a) original sliver platelets with average thickness of 5.5 ± 1 nm, the inset is side view of platelets; (b) thickened platelets (15 ± 2 nm) after 50% of new silver added relative to that originally present in platelets; (c) small cubes (18 ± 1.5 nm) and bipyramids (22 ± 2 nm) after 250% new silver added; (d) larger cubes (23 ± 2 nm) and bipyramids (29 ± 4 nm) after 600% of new silver added. The scale bar is 100 nm for (a), 20 nm for inset in (a), and 50 nm for (b), (c) and (d).

Already formed cubes and bipyramids increase in size very slightly at this stage (less than *ca.* 10%) until all the platelets are converted. Sometimes, a double structure of the peaks can be resolved, which is consistent with the coexistence of small cubes and bipyramids and thickened platelets.

Upon further silver addition to the system after complete platelet conversion, cubes and bipyramids can be enlarged with perfect shape preservation (Fig. 1). The growth can be performed smoothly to *ca.* 100 nm cubes (3 stages of 300% addition on top of initial 600% silver added to original platelets). In the course of the regrowth, the plasmonic peak shifts continuously to larger wavelengths from 407 to *ca.* 480 nm (Fig. 2b) for NPs reaching *ca.* 100 nm (Fig. 1c). At this time, a double peak is observed in the spectra due to resolved plasmonic resonances of larger cubes and bipyramids.

Based on our evidence on the transformation pathway and the reported results for the formation of silver bipyramids[8,14] and defect elucidation in platelets,[11] a schematic model presented in Fig. 4 can be proposed. The deciding factor for the formation of bipyramids (Fig. 4a) is either a single planar twinning defect or, more generally (and more likely), an odd number of multiple joint twinning planes.[11] The second necessary criterion for shape selection is specific regrowth conditions, which promote formation of (100) facets. It is established that the presence of PVP and high temperatures favour formation of these facets.[14,15] The cube formation is essentially analogous to the formation of the bipyramids. The only crucial difference is an even number of planar twinning defects that effectively cancel each other in terms of an overall effect on NP morphology leading to a shape formed by defect-free lattices (Fig. 4b). It is important to note that the twinning defects in the plane of the cube body diagonals are observed in the vast majority of the cubes (Fig. 1a,d). The defects are irregular and extensive multiple twinning as

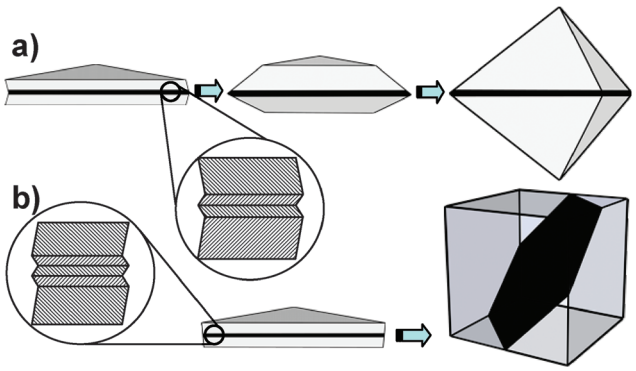

Fig. 4 Schematic transformation pathways: (a) silver platelets with odd number of twinned defects convert to right bipyramids; (b) silver platelets with even number of twinned defects convert to twinned cubes.

described in the literature[11] (not 2 or 3 planes as shown for simplicity in Fig. 4). Detailed studies of the defects by HR-TEM are currently in progress to elucidate the diverse nature of multiple twinning.

As can be deduced, the formation of the cubes geometrically requires hexagonal platelets as a base (Fig. 4b). In this respect, we have attempted to find a correlation between the fraction of hexagonal platelets initially and cubes in the final mixture. Based on more than 50 independent experiments we could not establish such correlation. In fact, in the earlier transformation stages a progressively larger fraction of truncated triangular platelets was observed (Fig. S3†) that clearly indicated that platelet shape changes significantly during the transformation. At the same time, upon further transformation a significant portion of the hexagonal platelets converted into right-angle bipyramids being driven by the underlying structural determinant of an odd number of multiple twinned defects. Hexagonal bipyramids were not observed during the transformation, since minimization of the number of facets, and hence the surface area, is energetically favourable. Therefore, the nature of the planar twinning defect in the platelets, and not the shape of the platelets, determines the outcome of the transformation. The relative amounts of cubes and bipyramids remain constant for the same batch of precursor platelets and vary appreciably from batch to batch. Several systematic variations in the platelet preparation did not afford a control over the defect nature. One potentially promising direction for such a control is based on exploring further platelet aging as a factor. Older weathered platelet dispersions were consistently observed yielding a slightly larger fraction of cubes compared with the freshly prepared platelets.

The discussed silver cubes and right bipyramids are prepared by a facile reproducible method in aqueous solution and should prove useful by virtue of their simple shape control and tunability of optical properties. For instance, hollow gold cages can be readily produced based on these NPs.[16] Furthermore, bipyramids have been proposed as especially promising for applications requiring sharp corners,[8] such as surface-enhanced Raman scattering (SERS).[17] To that effect we evaluated the efficiency of the cubes and bipyramids as a SERS substrate in comparison with other AgNP morphologies. Cubes and bipyramids proved to be very effective in SERS (Fig. S4 in ESI†), significantly more so than platelets, and second only to decahedral AgNPs (the best NP shape for SERS we have tested so far[7b]). In this respect, pure right bipyramids are expected to feature SERS efficiency comparable with decahedra and other bipyramids.[18]

Current work in this project is focused on the improvement of size-dispersity of cubes and right bipyramids through the refinement of the platelet preparation. An additional direction is to understand and control the factors affecting the selectivity toward formation of cubes and bipyramids.

In conclusion, we described and elucidated transformation pathways of silver platelets to right bipyramids and twinned cubes. A model of this structural transformation is presented, based on direct electron microscopy evidence and UV-vis spectroscopic data. Preservation of odd- and even-number of multiple planar twinned defects in the platelets and stabilization of {100} planes are necessary prerequisites for the reproducible formation of the described nanoshapes.

The authors gratefully acknowledge financial support from NSERC, CFI, OIT, Research Corp. and WLU. Philip Scott is acknowledged for contribution in the initial stages of the project. The Centre for Nanostructure Imaging (University of Toronto) is greatly appreciated for access to electron microscopy. The authors thank Neil Coombs for assistance with HR-TEM.

Notes and references

1 M. P. Pileni, *J. Phys. Chem. C*, 2007, **111**, 9019.
2 C. Burda, X. B. Chen, R. Narayanan and M. A El-Sayed, *Chem. Rev.*, 2005, **105**, 1025.
3 X. H. Huang, P. Jain, I. H. El-Sayed and M. A. El-Sayed, *Nanomedicine (London, UK)*, 2007, **2**, 681.
4 S. Lal, S. Link and N. J. Halas, *Nat. Photonics*, 2007, **1**, 641.
5 A. R. Tao, S. Habas and P. Yang, *Small*, 2008, **4**, 310.
6 Y. Sun, B. Gates, B. Mayers and Y. Xia, *Nano Lett.*, 2002, **2**, 165.
7 (*a*) A. Sanchez-Iglesias, I. Pastoriza-Santos, J. Perez-Juste, B. Rodriguez-Gonzalez, F. J. G. de Abajo and L. M. Liz-Marzan, *Adv. Mater.*, 2006, **18**, 2529; (*b*) B. Pietrobon and V. Kitaev, *Chem. Mater.*, 2008, **20**, 5186.
8 B. J. Wiley, Y. J. Xiong, Z. Y. Li, Y. D. Yin and Y. N. Xia, *Nano Lett.*, 2006, **6**, 765.
9 C. Lofton and W. Sigmund, *Adv. Funct. Mater.*, 2005, **15**, 1197.
10 (*a*) R. C. Jin, Y. Cao, E. C. Hao, G. S. Metraux, G. C. Schatz and C. A. Mirkin, *Nature*, 2003, **425**, 487; (*b*) R. C. Jin, Y. Cao, C. A. Mirkin, K. L. Kelly, G. C. Schatz and J. G. Zheng, *Science*, 2001, **294**, 1901.
11 D. Aherne, D. M. Ledwith, M. Gara and J. M. Kelly, *Adv. Funct. Mater.*, 2008, **18**, 2005.
12 (*a*) C. Xue, G. S. Metraux, J. E. Millstone and C. A. Mirkin, *J. Am. Chem. Soc.*, 2008, **130**, 8337; (*b*) X. Wu, P. L. Redmond, H. Liu, Y. Chen, M. Steigerwald and L. Brus, *J. Am. Chem. Soc.*, 2008, **130**, 9500.
13 F. Gao, Q. Lu and S. Komarneni, *Chem. Mater.*, 2008, **17**, 856.
14 B. J. Wiley, Y. Sun and Y. Xia, *Acc. Chem. Res.*, 2007, **40**, 1067.
15 N. R. Jana, L. Gearheart and C. J. Murphy, *Chem. Commun.*, 2001, 617.
16 S. E. Skrabalak, L. Au, X. D. Li and Y. Xia, *Nat. Protocols*, 2007, **2**, 2182.
17 J. A. Dieringer, A. D. McFarland, N. C. Shah, D. A. Stuart, A. V. Whitney, C. R. Yonzon, M. A. Young, X. Y. Zhang and R. P. Van Duyne, *Faraday Discuss.*, 2006, **132**, 9.
18 M. Z. Liu and P. Guyot-Sionnest, *J. Phys. Chem. B*, 2005, **109**, 22192.